ACS APPLIED OPTICAL MATERIALS

pubs.acs.org/acsaom
Letter

DNA-Guided Self-Assembly of Carbon Nanotubes and Quantum Dots

Durham Smith* and Grigory Tikhomirov*

Cite This: ACS Appl. Opt. Mater. 2025, 3, 569−574
Read Online

ACCESS | Metrics & More | Article Recommendations | Supporting Information

ABSTRACT: The ability to robustly and with scalability detect single photons in the visible spectrum with wavelength resolution would transform many imaging applications. Theoretical studies propose an array of carbon nanotubes (CNTs) functionalized with semiconductor quantum dots (QDs) as a physical realization of such photon sensors. In this work, we report approaches to synthesize these CNT-QD nanostructures using DNA as a smart glue to connect CNTs to QDs.

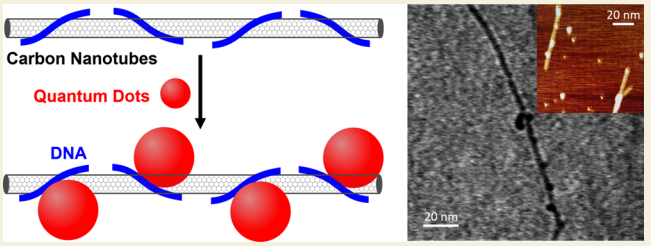

KEYWORDS: *carbon nanotubes, quantum dots, self-assembly, photon sensors, DNA*

Detecting single photons is essential for numerous applications.[1] Integrating frequency resolution into this detection process can enable new capabilities from capturing galaxies[2] parsecs away to resolving fast nanoscale processes in our own cells.[3,4] The ultimate goal in photon sensing technology is the development of a device capable of operating at room temperature and discerning both photon intensity and spectrum with single photon sensitivity. Despite its significant potential, this level of technological advancement in photon detection has yet to be realized.

In this work, we describe an approach to construct a component for nanoscale single photon sensors by leveraging DNA-programmed self-assembly of semiconductor quantum dots (QDs) and carbon nanotubes (CNTs). When QDs are placed close enough to semiconducting CNTs, an exciton generated upon a photon absorption by a QD can nonradiatively transfer onto CNT. This transfer can be detected as a change in electronic transport in a field effect transistor, where a semiconducting CNT serves as the channel material. This proposed architecture is theorized to enable single photon detection with frequency identification, characterized by low dark counts, minimal jitter, picosecond response times, and room-temperature operation, while also being scalable to megapixels.[5]

Toward this goal, we synthesized DNA-functionalized QDs and DNA-functionalized CNTs, and then used QDs to hybridize CNTs via partially complementary DNA strands. The frequency resolution of the device can be achieved with QDs of varying bandgap energies. The bandgap can be readily controlled via reaction time. We have previously reported DNA-based programming of quantum dot valency, self-assembly, and luminescence where DNA can be used both to program bandgap and enable DNA functionalization.[6] Furthermore, DNA has been shown to be able to solubilize[7] and separate[8] CNTs by chirality type while retaining the capacity to hybridize with other DNA strands, enabling integration into DNA nanostructures.[9,10] Moreover, electrodes can be effectively fabricated at the ends of CNTs assembled in this manner,[11] allowing, in principle, scalable construction of photon sensors.

We synthesized CdTe QDs in an aqueous reaction of $CdCl_2$ with sodium hydrogen telluride (NaHTe) using mercaptopropionic acid (MPA) as a capping ligand adapting a published protocol[12] (Figure 1a). Longer reaction times lead to smaller bandgaps and thus longer luminescence wavelengths (Figure 1c) due to the growing diameter of QDs and diminishing quantum confinement.[6] To create QDs that can hybridize to CNTs we synthesized QDs bearing a DNA strand[6] (Supporting Information Sections 1−4). Their synthesis follows that of MPA-capped QDs but uses modified DNA in addition to MPA. This DNA strand consists of a normal phosphodiester segment for hybridization with DNA-wrapped CNTs and a phosphorothioate segment for the attachment to the CdTe QD[13] (Figures 1b and 2b). There exist a number of other strategies for anchoring DNA to nanoparticles, such as oligo-histidine linked to DNA or peptide nucleic acid (PNA),[14] as well as poly-A DNA.[15] In this work we chose to use DNA-only anchors that were previously shown to be compatible with CdTe QDs[6] and can be produced cost-efficiently at scale.

We synthesized CNTs functionalized with DNA by adapting a published protocol (Figure 2).[16] Briefly, we sonicated CNT

Special Issue: Optical Applications of DNA Nanotechnology

Received: December 31, 2024
Revised: February 19, 2025
Accepted: February 20, 2025
Published: February 21, 2025

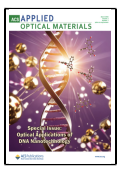

https://doi.org/10.1021/acsaom.4c00534
ACS Appl. Opt. Mater. 2025, 3, 569−574

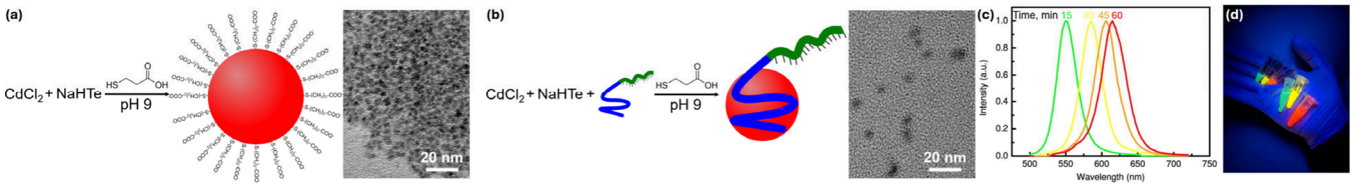

Figure 1. Synthesis of DNA functionalized CdTe QDs. (a) Synthesis of mercaptopropionic acid (MPA)-capped CdTe QDs and corresponding representative transmission electron microscopy (TEM) image. (b) Synthesis of DNA-functionalized MPA-capped QDs. Blue portion indicates DNA strand with phosphorothioate backbone, green portion indicates normal phosphate backbone, black lines indicate bases available for hybridization (see Figure 2 for their structures). During drying on O_2-plasma activated carbon film of TEM grid, QDs typically aggregate when functionalized with MPA only and disperse well when functionalized with both MPA and DNA. (c) Example luminescence spectra at different synthesis times. (d) Example luminescence of MPA-capped QDs samples without (left three tubes) and with DNA (right three tubes) for four different bandgaps visualized with 254 nm UV light source. An intermediate (orange) spectrum is added to demonstrate a slowdown in the growth rate of the QDs. The four spectra were taken every 15 min since the beginning of reaction.

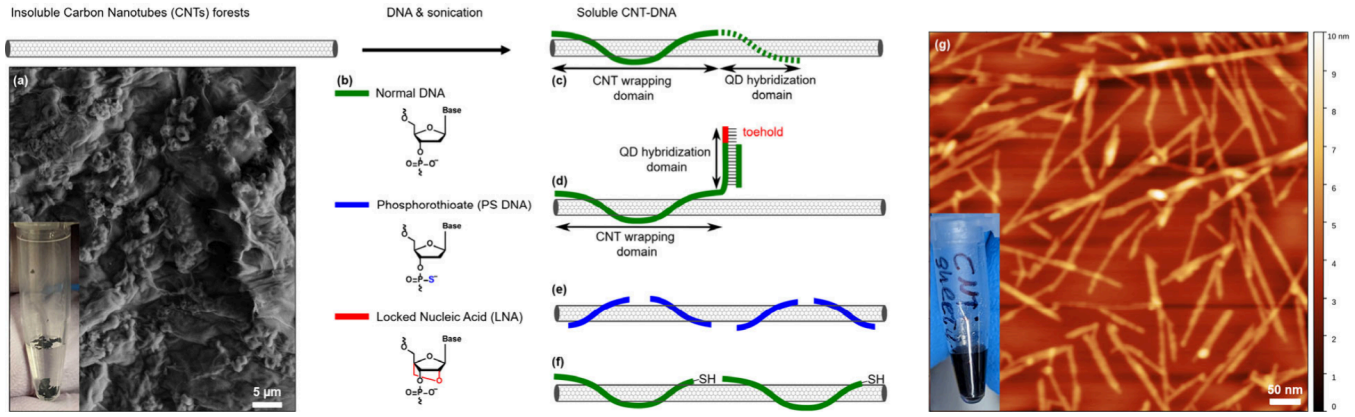

Figure 2. Synthesis of DNA-functionalized CNTs. (a) Example scanning electron microscopy image of insoluble CNT flake from Nanointegris. (b) Three DNA types used in this work. (c) Schematic representation of DNA strands used for direct hybridization with DNA-functionalized QDs. (d) DNA strands used for TMSD with DNA-functionalized QDs. (e) DNA strands used for PS-mediated attachment to QDs. (f) DNA strands used for thiol-mediated attachment to QDs. (g) Example AFM image of DNA-functionalized and purified CNTs showing single tubes along with CNT bundles. Insets in (a) and (g) show actual samples of insoluble and DNA-solubilized CNTs.

films with DNA, followed by purification (see S5−S7 for protocols and S9 for DNA sequences). Bundled single-walled carbon nanotubes are effectively dispersed in water by sonication in the presence of single-stranded DNA (ssDNA). DNA can bind to carbon nanotubes through π-stacking, resulting in helical wrapping to the surface with the binding free energy of ssDNA to carbon nanotubes exceeding that of two nanotubes for each other.[7] We explored four approaches, each using a different type of DNA.

Approach 1

We used normal DNA comprised of two domains: (a) A 40-nucleotide GT-rich domain that is reported to have strong affinity for CNT surface[7] and (b) A 16-nucleotide domain for binding DNA-functionalized QDs via DNA-hybridization (Figure 2c). The 16-nucleotide sequence was designed using NUPACK[17] to minimize secondary structures and spurious interactions with other DNA strands used here. While DNA functionalization resulted in well-dispersed CNTs (Figure 3g), attaching QDs to these DNA-functionalized CNTs results in low yields of QD attachment (Figures 3a and S10), likely caused by the strong interaction of the 16-nucleotide domain with the CNT surface. One potential solution would be to try several other DNA sequences hoping that some will have weaker binding to CNT surface. However, there are no existing models that predict arbitrary DNA sequence binding to carbon nanotubes. Therefore, we next explored a more rational alternative, approach 2.

Approach 2

We used a DNA strand comprised of three segments: a 41-nucleotide CNT-wrapping region, a 15-nucleotide region complementary to the displaced strand, and a 5-nucleotide toehold domain of locked nucleic acids (Figure 2d). We introduced the double-stranded region to minimize adsorption onto the CNTs sidewall in order to mitigate the slower hybridization kinetics of DNA wrapped around CNTs[18] and to reduce electrostatic repulsion between the CNT and QD. We introduced a toehold to subsequently replace the shorter partner strand in the complex with a DNA-functionalized QD via toehold-mediated strand displacement (TMSD).[10] The toehold was designed with Locked Nucleic Acid (LNA) modification that has stronger affinity to DNA compared to unmodified DNA due to reduction of the entropic contribution during the hybridization process[19] (Figure 2b). However, we found that both the preformed double-stranded DNA complex and the single LNA-modified strand failed to disperse CNTs and yielded entangled networks of CNTs (Figures 3b and S5−S7).

Approach 3

To create simpler anchors for QD attachment on CNTs we used DNA strands with a phosphorothioate backbone leveraging cadmium's affinity for the sulfide in the PS DNA (Figure 2e). Short (6-nucleotide) PS strands were effective in maximizing CNT dispersion as previously reported, albeit without phosphorothioate backbones.[16] We found that the addition of

https://doi.org/10.1021/acsaom.4c00534
ACS Appl. Opt. Mater. 2025, 3, 569−574

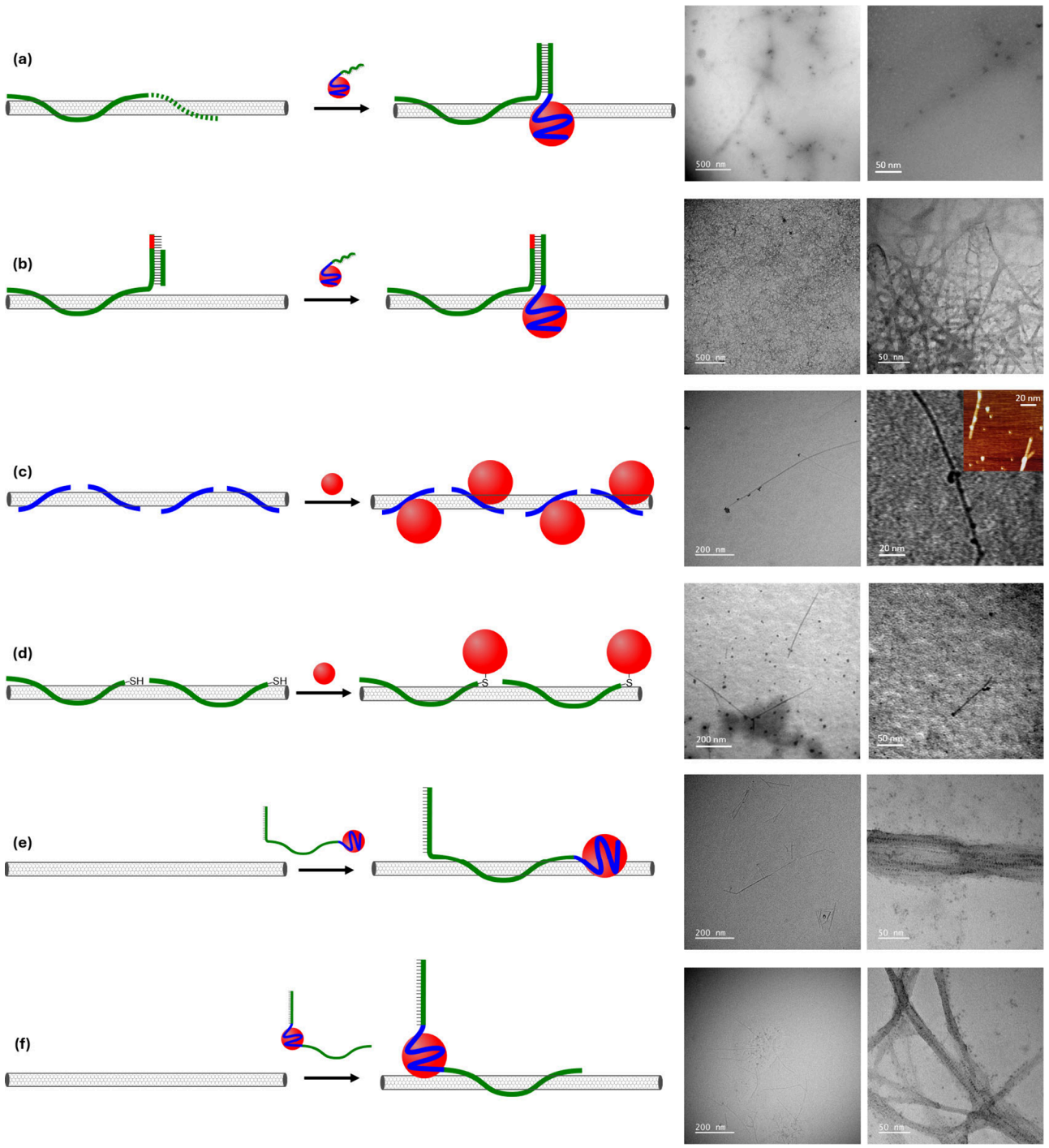

Figure 3. Assembly of CNT-QDs. (a) Direct hybridization with DNA-functionalized QDs. (b) Attachment of QDs via TMSD with monovalent DNA-functionalized QDs. (c) PS-mediated attachment to QDs. Inset shows a taping mode Atomic Force Microscopy image of CNTs functionalized with QDs. (d) Covalent functionalization between unmodified QDs. (e, f) Solubilization of CNTs using DNA-functionalized QD.

phosphorothioated backbones in these strands did not affect their ability to solubilize CNTs, although solubilized CNT exhibited more bundling than the samples solubilized with longer strands (S13).

Approach 4

We used DNA strands with a thiol modification at the 3′ (Figure 3f) end to solubilize CNTs and form covalent QD-DNA assemblies.[20] Thiol-modified 10-nucleotide poly-T strands in their oxidized (disulfide) form were found to solubilize CNTs effectively. However, upon reduction with tris(2-carboxyethyl)-phosphine hydrochloride (TCEP), they lost their ability to solubilize CNTs, likely due to reoxidation by air oxygen that leads to cross-linking of CNTs via DNA termini S−S bridges. These results underscore the complexity of the interplay between DNA modifications and their interactions with CNTs, influencing the effectiveness of solubilization and subsequent QD attachment.

We explored five distinct strategies for conjugating QDs to CNTs.

https://doi.org/10.1021/acsaom.4c00534
ACS Appl. Opt. Mater. 2025, 3, 569−574

Strategy 1

We first tried to perform a DNA-mediated hybridization between QDs and CNTs. We used QDs and CNTs both functionalized with DNA, Figure 3a. We quantified the concentrations of QDs and CNTs via ultraviolet−visible (UV−vis) extinction spectroscopy and mixed them in a 1:100 CNT:QD ratio. To alleviate electrostatic repulsion between negatively charged QDs and DNA-wrapped CNTs, we used elevated concentrations of Mg^{2+} and Na^{+}. We annealed reaction mixtures as previously reported[6] (S11). This strategy yielded sparse and nonuniform distribution of QDs on CNTs (Figures 3 and S11). We observed inconsistent dispersion of QDs around CNTs and significant QD aggregation, which might be related to the loss of MPA ligands during purification observed previously.[12] We hypothesized that poor formation of CNT-QD hybrids was due to strong electrostatic repulsion between the negatively charged DNA on CNTs and MPA passivation ligands on QDs, potentially compounded by DNA adsorption on CNT sidewalls.[18]

Strategy 2

To overcome the limitations of strategy 1, we adopted a double-stranded linker complex strategy.[10] CNTs were solubilized with a complex containing a double-stranded DNA linker (Figure 3b). This was followed by a toehold-mediated strand displacement of the strand not directly interacting with the CNT with a strand conjugated to a monovalent quantum dot, leading to either a zip or a classical bond formation (Figure 3b, where only a zip bond bringing QD close to CNT is shown). We discovered that locked nucleic acid (LNA) toeholds in the DNA strands used for CNT solubilization resulted in significant aggregation of CNTs and their QD conjugates, likely due to the strong spurious multivalent binding of LNA toeholds.

Strategy 3

We used DNA strands with phosphorothioate backbones to solubilize CNTs, which were then combined with MPA-coated CdTe QDs and annealed (Figures 3c and S13). It is worth noting that DNA strands orient to stack with the surface of the nanotube. This places the phosphates on the periphery available to bind to QDs.[7] We successfully identified individual CNT-QD structures. The purified CNT-QD solutions display very weak luminescence observed for strategies 1 and 2, likely due to non-irradiative exciton transfer from QDs to CNTs (Figure 4). The control experiment with the same concentrations of CNTs and QDs where MPA-capped QDs lack the means to attach to CNTs showed similar absorbance values, while there was ∼50 higher luminescence intensity. The remnant luminescence in the CNT-QD sample is likely to stray QDs unattached to CNTs that are always observed in small amounts in TEM even after purification. These findings mark the first demonstration that phosphorothioate DNA can effectively be used to attach CdTe QDs to CNTs.

Strategy 4

We also investigated the covalent functionalization between unmodified QDs and DNA-coated CNTs. Here, we solubilized CNTs using DNA strands modified with thiol groups at their 3′ ends and then combined them with MPA-functionalized CdTe QDs (Figures 3d and S14). Interestingly, we found that CNTs were effectively solubilized only when thiolated DNA strands were in their unreduced state. In attempts to combine these DNA-wrapped CNTs with QDs, we experimented with both the unreduced state of these strands and the reduction via TCEP

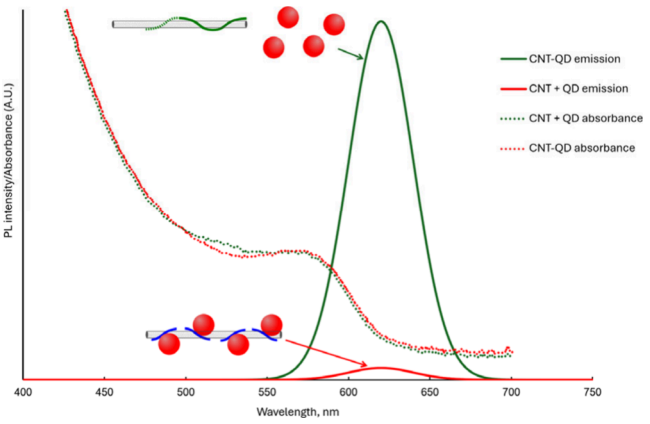

Figure 4. Absorption spectra (dotted lines) and photoluminescence spectra (solid lines) of CNT-DNA assemblies obtained by Strategy 3 in red. The corresponding spectra for mixture of CNTs and quantum dots before self-assembly is shown in green displaying similar absorbance values but much lower luminescence intensity presumably due to non-irradiative exciton transfer from QDs to CNTs. Our UV−vis instrument has a range of 200−700 nm, and the spectrometer can record emission in 400−750 nm range. CNT-QD assemblies with red QDs from Strategy 3 with maximum emissions at 622 nm were used for the spectra recording. The residual photoluminescence is likely due to QDs unattached to CNTs. The concentration of CDs and CNTs was kept the same for the two samples.

after DNA-wrapping. While this approach was successful in forming CNT-QD hybrids, the density of QDs on the CNTs was notably low (Figures 3d and S14). This observation aligns with reports for CdSe/ZnS core/shell QDs.[20] It is also possible that QDs are attached to the CNT due to dissociation of DNA from the CNT surface, and multiple DNAs are acting as the ligands to stabilize the QD.

Strategy 5

To assemble photon sensor arrays with spectral resolution, QD-CNTs bearing QDs with different bandgaps need to be colocalized to the same pixel of a device. Toward this goal we functionalized CNTs with QDs that bear DNA strands that have an additional region for hybridization to DNA origami surface[9,10] (Figure 3e,f). These strands are comprised of a 10-nucleotide phosphorothioate segment for QD binding during synthesis, a 40-nucleotide segment for CNT wrapping, and a 20-nucleotide segment for hybridizing with DNA origami canvases.[21−23] These origamis can then be placed in precise locations and orientations onto lithographically defined patches.[24] Two variations in the positioning of these domains were tested: with QD-binding domain between the other domains (Figure 3e) and at the 3′ end of the strand (Figure 2f).

The latter may be more accessible to QD attachment compared with the former. In this sample luminescence quenching was observed, suggesting nonradiative energy transfer between QDs or between QDs and CNTs. We first synthesized monovalent QDs using the aforementioned DNA strand followed by the separation of unbound DNA (S12). These QDs were then used to solubilize the CNTs. Two designs gave different results. When located at the strand's end we observed the formation of CNT-QD hybrids, though with significant aggregation attributed to QD clustering and potential DNA hybridization (Figures 2e, S12). When the QD-binding domain was placed between the other two regions, CNTs were successfully solubilized, but many fewer QDs were visible in

https://doi.org/10.1021/acsaom.4c00534
ACS Appl. Opt. Mater. 2025, 3, 569−574

TEM imaging (Figures 2f, S12). We suspect that the sonication step in CNT solubilization might have degraded the QDs. In this sample luminescence quenching was also observed (spectrum not shown as it was just a baseline); however, the lack of QDs when TEM imaging suggests this is due to the destruction of QDs.

Strategy 6

We also explored the growth of QDs directly on CNTs. Here we grew lead sulfide (PbS) QDs on DNA-wrapped CNTs, utilizing the negatively charged backbone of DNA as a nucleation site for Pb^{2+} ions.[25] While successful in forming CNT-QD composites, the process resulted in significant aggregation (S15), did not allow precise bandgap control of QDs, and lacked an effective method for integrating the CNT-QD constructs into arrays for multifrequency photon sensor applications.

The current methodologies for attaching QDs to CNTs face several critical limitations. These include the inability to control QD density on CNTs effectively, the aggregation of CNT-QD hybrid nanostructures, the failure of the resulting nanocomposites to hybridize with other DNA structures for self-assembly, the excessive distance between CNTs and QDs impeding exciton transfer, and the modification of CNT sidewalls, which may disrupt their conductive properties.

We have tested several existing and developed several new strategies for assembling CNT-QD architectures. Notably, the noncovalent functionalization of DNA-coated CNTs with unmodified QDs (Strategy 3) and the use of DNA-functionalized QDs for solubilizing CNTs (Strategy 5) demonstrated improved QD density compared to published approaches. In addition, Strategy 5 adds a DNA handle for further attachment of CNT-QDs to DNA origami. Immobilization of CNTs-QDs on origami can enable self-assembly of CNT-QDs functionalized with QDs with several bandgaps for spectrally resolved photon sensing.

The aggregation of CNT components and resulting CNT-QDs architectures is still a recurring challenge. One way to mitigate aggregation is to use shorter CNTs, which can be achieved by extending sonication times. Shorter tubes will have less capabilities for tube−tube interaction, no matter what the nature of that interaction may be—van der Waals CNT-CNT, DNA−DNA, sulfur−sulfur, etc. To further reduce the persistent CNT aggregation one potential solution is prearranging CNTs in DNA trenches[9] before QD introduction. Furthermore, the observed aggregation of QDs over time indicates the necessity for more stable QD formulations, a crucial focus for future research to enhance QD-CNT functionalization.

Future work could explore longer DNA strands with phosphodiester and phosphorothioate regions, offering control over QD density and enabling hybridization and incorporation into photon sensor arrays. In addition, we are pursuing direct CNT functionalization of isolated suspended on chip array CNTs in collaboration with Aligned Carbon, Inc.

The CNT-QD assemblies reported here represent a small yet significant step toward the development of advanced photodetectors capable of detecting both light intensity and frequency. The DNA-guided noncovalent functionalization of CNTs with CdTe quantum dots opens new avenues for sophisticated light detection technologies, promising wide-ranging applications in scientific and technological fields.

■ ASSOCIATED CONTENT

Supporting Information

The Supporting Information is available free of charge at https://pubs.acs.org/doi/10.1021/acsaom.4c00534.

Synthesis and sample preparation protocols, additional atomic force and transmission electron microscopy images (PDF)

■ AUTHOR INFORMATION

Corresponding Authors

Durham Smith − *Department of Electrical Engineering and Computer Sciences, University of California Berkeley, Berkeley, California 94720, United States*; Email: durham@berkeley.edu

Grigory Tikhomirov − *Department of Electrical Engineering and Computer Sciences, University of California Berkeley, Berkeley, California 94720, United States*; orcid.org/0000-0001-6061-3843; Email: gt3@berkeley.edu

Complete contact information is available at: https://pubs.acs.org/10.1021/acsaom.4c00534

Notes

The authors declare no competing financial interest.

■ ACKNOWLEDGMENTS

We thank the members of the LBNL-SNL-UC Berkeley "Co-Design and Integration of nano-sensors on CMOS" and "Nanoscale hybrids: a new paradigm for energy-efficient optoelectronics" collaborations for useful discussions. This work was supported by U.S. Department of Energy, Office of Science, NSF DMR (2211148), NSF CAREER (2240000), and NSF POSE Phase 2 (2346048).

■ REFERENCES

(1) Chunnilall, C. J.; Degiovanni, I. P.; Kück, S.; Müller, I.; Sinclair, A. G. Metrology of single-photon sources and detectors: a review. *Opt. Eng.* **2014**, *53*, 081910.

(2) DESI Collaboration; Aghamousa, A.; et al. The DESI Experiment Part II: Instrument Design. *arXiv* DOI: 10.48550/arXiv.1611.00037 2016.

(3) Niwa, K.; Hattori, K.; Fukuda, D. Few-Photon Spectral Confocal Microscopy for Cell Imaging Using Superconducting Transition Edge Sensor. *Front. Bioeng. Biotechnol.* **2021**, *9*. DOI: 10.3389/fbioe.2021.789709

(4) Gao, L.; Smith, R. T. Optical hyperspectral imaging in microscopy and spectroscopy − a review of data acquisition. *J. Biophotonics* **2015**, *8*, 441−456.

(5) Young, S. M.; Sarovar, M.; Léonard, F. Nanoscale architecture for frequency-resolving single-photon detectors. *Commun. Phys.* **2023**, *6*, 1−9.

(6) Tikhomirov, G.; et al. DNA-based programming of quantum dot valency, self-assembly and luminescence. *Nat. Nanotechnol.* **2011**, *6*, 485−490.

(7) Zheng, M.; et al. DNA-assisted dispersion and separation of carbon nanotubes. *Nat. Mater.* **2003**, *2*, 338−342.

(8) Zheng, M.; et al. Structure-Based Carbon Nanotube Sorting by Sequence-Dependent DNA Assembly. *Science* **2003**, *302*, 1545−1548.

(9) Sun, W.; et al. Precise pitch-scaling of carbon nanotube arrays within three-dimensional DNA nanotrenches. *Science* **2020**, *368*, 874−877.

(10) Maune, H. T.; et al. Self-assembly of carbon nanotubes into two-dimensional geometries using DNA origami templates. *Nat. Nanotechnol.* **2010**, *5*, 61−66.

(11) Zhao, M.; et al. DNA-directed nanofabrication of high-performance carbon nanotube field-effect transistors. *Science* **2020**, *368*, 878−881.
(12) Li, L.; Qian, H.; Fang, N.; Ren, J. Significant enhancement of the quantum yield of CdTe nanocrystals synthesized in aqueous phase by controlling the pH and concentrations of precursor solutions. *J. Lumin.* **2006**, *116*, 59−66.
(13) Pecoraro, V. L.; Hermes, J. D.; Cleland, W. W. Stability constants of magnesium and cadmium complexes of adenine nucleotides and thionucleotides and rate constants for formation and dissociation of magnesium-ATP and magnesium-ADP. *Biochemistry* **1984**, *23*, 5262−5271.
(14) Green, C. M.; et al. Direct and Efficient Conjugation of Quantum Dots to DNA Nanostructures with Peptide-PNA. *ACS Nano* **2021**, *15*, 9101−9110.
(15) Yao, G.; et al. Programming nanoparticle valence bonds with single-stranded DNA encoders. *Nat. Mater.* **2020**, *19*, 781−788.
(16) Vogel, S. R.; Kappes, M. M.; Hennrich, F.; Richert, C. An Unexpected New Optimum in the Structure Space of DNA Solubilizing Single-Walled Carbon Nanotubes. *Chem. - Eur. J.* **2007**, *13*, 1815−1820.
(17) Zadeh, J. N.; et al. NUPACK: Analysis and design of nucleic acid systems. *J. Comput. Chem.* **2011**, *32*, 170−173.
(18) Jeng, E. S.; Barone, P. W.; Nelson, J. D.; Strano, M. S. Hybridization Kinetics and Thermodynamics of DNA Adsorbed to Individually Dispersed Single-Walled Carbon Nanotubes. *Small* **2007**, *3*, 1602−1609.
(19) Owczarzy, R.; You, Y.; Groth, C. L.; Tataurov, A. V. Stability and Mismatch Discrimination of Locked Nucleic Acid−DNA Duplexes. *Biochemistry* **2011**, *50*, 9352−9367.
(20) Campbell, J. F.; Tessmer, I.; Thorp, H. H.; Erie, D. A. Atomic Force Microscopy Studies of DNA-Wrapped Carbon Nanotube Structure and Binding to Quantum Dots. *J. Am. Chem. Soc.* **2008**, *130*, 10648−10655.
(21) Tikhomirov, G.; Petersen, P.; Qian, L. Fractal assembly of micrometre-scale DNA origami arrays with arbitrary patterns. *Nature* **2017**, *552*, 67−71.
(22) Tikhomirov, G.; Petersen, P.; Qian, L. Programmable disorder in random DNA tilings. *Nat. Nanotechnol.* **2017**, *12*, 251−259.
(23) Tikhomirov, G.; Petersen, P.; Qian, L. Triangular DNA Origami Tilings. *J. Am. Chem. Soc.* **2018**, *140*, 17361−17364.
(24) Gopinath, A.; et al. Absolute and arbitrary orientation of single-molecule shapes. *Science* **2021**, *371*, No. eabd6179.
(25) Ye, Q.; et al. Solution-Processable Carbon Nanotube Nanohybrids for Multiplexed Photoresponsive Devices. *Adv. Funct. Mater.* **2021**, *31*, 2105719.

https://doi.org/10.1021/acsaom.4c00534
ACS Appl. Opt. Mater. 2025, 3, 569−574